inhibited the increase in TXB_2 level in BAL fluid. Thus one of the possible mechanisms by which ONO-1301 attenuates lung inflammation may be mediated by inhibition of TXA_2 synthesis. A recent study has shown that a TXA_2 receptor agonist enhances the expression of adhesion molecules by human vascular endothelial cells (12). In the present study, ONO-1301 significantly inhibited ICAM-1 and VCAM-1 expression in the bleomycin-treated lung. Adhesion molecules including ICAM-1 and VCAM-1 have been shown to contribute to bleomycin-induced pulmonary fibrosis by mediating the accumulation of leukocytes (9, 16, 19, 23). These findings suggest that ONO-1301 may attenuate lung inflammation at least in part through inhibition of ICAM-1 and VCAM-1 expression.

Lung fibroblasts play an important role in the development of fibrosis in the lung (22, 25, 31). Prostaglandins are known to have various functions on lung fibroblasts via an elevation of intracellular cAMP level (3, 14–17). In the present study, a single subcutaneous administration of ONO-1301 significantly increased plasma cAMP level in mice. In vitro studies demonstrated that ONO-1301 dose-dependently increased intracellular cAMP level in mouse lung fibroblasts and that this compound dose-dependently inhibited fibroblast proliferation. The inhibitory effect of ONO-1301 was reproduced by 8-bromo cAMP, a cAMP analog, and attenuated by a PKA inhibitor. These results suggest that ONO-1301 directly inhibits fibroblast proliferation at least in part through activation of the cAMP/PKA pathway. Dussaubat et al. (5) have demonstrated that imidazole, a thromboxane synthesis inhibitor, decreases bleomycin-induced acute lung inflammation, but it does not affect pulmonary fibrosis at later points. In the present study, a prostacyclin analog, but not a thromboxane synthesis inhibitor, significantly reduced fibroblast proliferation. These results suggest that the inhibitory effect of ONO-1301 on fibroblast proliferation may be mediated mainly by its prostacyclin-like activity. TGF-β, especially TGF-β1 plays an important role in the pathogenesis of pulmonary fibrosis (7, 26, 32). In the present study, ONO-1301 did not significantly alter the active TGF-β1 level in BAL fluid. Previous studies have shown that a prostacyclin agonist suppresses TGF-β-induced connective tissue growth factor, a potent profibrotic mediator, expression in part through activation of the cAMP/PKA pathway (28, 29). Thus it is interesting to speculate that ONO-1301 attenuated the development of pulmonary fibrosis through suppression of connective tissue growth factor.

In the present study, ONO-1301 significantly improved survival in bleomycin-injected mice. ONO-1301 inhibited lung inflammation and lung fibroblast proliferation. As a result, ONO-1301 may have beneficial effects on survival in bleomycin-injected mice. Unfortunately, we could not observe significant differences in fibrotic changes between the Vehicle group and ONO-1301 group when we administered ONO-1301 after fibrosis was established. These results imply that ONO-1301 may be insufficient to reverse established pulmonary fibrosis.

In conclusion, subcutaneous administration of ONO-1301, a novel long-lasting prostacyclin agonist, attenuated the development of bleomycin-induced pulmonary fibrosis and improved survival in mice. The beneficial effects were mediated at least in part by inhibition of TXA_2 synthesis and activation of the cAMP/PKA pathway. Thus administration of this compound may be a new therapeutic strategy for the treatment of pulmonary fibrosis.

ACKNOWLEDGMENTS

The authors thank Yuki Isono, Natue Sakata, and Manami Sone for excellent technical assistance.

GRANTS

This work was supported by grants from Ono Pharmaceutical Co., Ltd.

REFERENCES

1. **Ashcroft T, Simpson JM, and Timbrell V.** Simple method of estimating severity of pulmonary fibrosis on a numerical scale. *J Clin Pathol* 41: 467–470, 1988.
2. **Chandler DB, Giri SN, Chen Z, and Hyde DM.** The in vitro synthesis and degradation of prostaglandins during the development of bleomycin-induced pulmonary fibrosis in hamsters. *Prostaglandins Leukot Med* 11: 11–31, 1983.
3. **Clark JG, Kostal KM, and Marino BA.** Bleomycin-induced pulmonary fibrosis in hamsters. An alveolar macrophage product increases fibroblast prostaglandin E2 and cyclic adenosine monophosphate and suppresses fibroblast proliferation and collagen production. *J Clin Invest* 72: 2082–2091, 1983.
4. **Cruz-Gervis R, Stecenko AA, Dworski R, Lane KB, Loyd JE, Pierson R, King G, and Brigham KL.** Altered prostanoid production by fibroblasts cultured from the lungs of human subjects with idiopathic pulmonary fibrosis. *Respir Res* 3: 17, 2002.
5. **Dussaubat N, Capetillo M, Lathrop ME, Mendoza R, and Oyarzun M.** The effects of imidazole on pulmonary damage induced by bleomycin. *Biol Res* 28: 261–266, 1995.
6. **Giri SN.** Novel pharmacological approaches to manage interstitial lung fibrosis in the twenty-first century. *Annu Rev Pharmacol Toxicol* 43: 73–95, 2003.
7. **Giri SN, Hyde DM, and Hollinger MA.** Effect of antibody to transforming growth factor beta on bleomycin induced accumulation of lung collagen in mice. *Thorax* 48: 959–966, 1993.
8. **Giri SN and Witt TC.** Effects of intratracheal administration of bleomycin on prostaglandins and thromboxane-B2 and collagen levels of the lung in hamsters. *Exp Lung Res* 9: 119–133, 1985.
9. **Hamaguchi Y, Nishizawa Y, Yasui M, Hasegawa M, Kaburagi Y, Komura K, Nagaoka T, Saito E, Shimada Y, Takehara K, Kadono T, Steeber DA, Tedder TF, and Sato S.** Intercellular adhesion molecule-1 and L-selectin regulate bleomycin-induced lung fibrosis. *Am J Pathol* 161: 1607–1618, 2002.
10. **Horio T, Nishikimi T, Yoshihara F, Matsuo H, Takishita S, and Kangawa K.** Inhibitory regulation of hypertrophy by endogenous atrial natriuretic peptide in cultured cardiac myocytes. *Hypertension* 35: 19–24, 2000.
11. **Huaux F, Liu T, McGarry B, Ullenbruch M, and Phan SH.** Dual roles of IL-4 in lung injury and fibrosis. *J Immunol* 170: 2083–2092, 2003.
12. **Ishizuka T, Kawakami M, Hidaka T, Matsuki Y, Takamizawa M, Suzuki K, Kurita A, and Nakamura H.** Stimulation with thromboxane A2 (TXA2) receptor agonist enhances ICAM-1, VCAM-1 or ELAM-1 expression by human vascular endothelial cells. *Clin Exp Immunol* 112: 464–470, 1998.
13. **Itoh T, Nagaya N, Fujii T, Iwase T, Nakanishi N, Hamada K, Kangawa K, and Kimura H.** A combination of oral sildenafil and beraprost ameliorates pulmonary hypertension in rats. *Am J Respir Crit Care Med* 169: 34–38, 2004.
14. **Kohyama T, Liu X, Kim HJ, Kobayashi T, Ertl RF, Wen FQ, Takizawa H, and Rennard SI.** Prostacyclin analogs inhibit fibroblast migration. *Am J Physiol Lung Cell Mol Physiol* 283: L428–L432, 2002.
15. **Kolodsick JE, Peters-Golden M, Larios J, Toews GB, Thannickal VJ, and Moore BB.** Prostaglandin E2 inhibits fibroblast to myofibroblast transition via E. prostanoid receptor 2 signaling and cyclic adenosine monophosphate elevation. *Am J Respir Cell Mol Biol* 29: 537–544, 2003.
16. **Li Y, Azuma A, Takahashi S, Usuki J, Matsuda K, Aoyama A, and Kudoh S.** Fourteen-membered ring macrolides inhibit vascular cell adhesion molecule 1 messenger RNA induction and leukocyte migration: role in preventing lung injury and fibrosis in bleomycin-challenged mice. *Chest* 122: 2137–2145, 2002.
17. **Liu X, Ostrom RS, and Insel PA.** cAMP-elevating agents and adenylyl cyclase overexpression promote an antifibrotic phenotype in pulmonary fibroblasts. *Am J Physiol Cell Physiol* 286: C1089–C1099, 2004.

18. Lotvall J, Elwood W, Tokuyama K, Sakamoto T, Barnes PJ, and Chung KF. A thromboxane mimetic, U-46619, produces plasma exudation in airways of the guinea pig. *J Appl Physiol* 72: 2415–2419, 1992.
19. Matsuse T, Teramoto S, Katayama H, Sudo E, Ekimoto H, Mitsuhashi H, Uejima Y, Fukuchi Y, and Ouchi Y. ICAM-1 mediates lung leukocyte recruitment but not pulmonary fibrosis in a murine model of bleomycin-induced lung injury. *Eur Respir J* 13: 71–77, 1999.
20. Murakami S, Nagaya N, Itoh T, Fujii T, Iwase T, Hamada K, Kimura H, and Kangawa K. C-type natriuretic peptide attenuates bleomycin-induced pulmonary fibrosis in mice. *Am J Physiol Lung Cell Mol Physiol* 287: L1172–L1177, 2004.
21. Murota SI, Morita I, and Abe M. The effects of thromboxane B2 and 6-ketoprostaglandin F1alpha on cultured fibroblasts. *Biochim Biophys Acta* 479: 122–125, 1977.
22. Kaminski N, Belperio JA, Bitterman PB, Chen L, Chensue SW, Choi AM, Dacic S, Dauber JH, Du Bois RM, Enghild JJ, Fattman CL, Grutters JC, Haegens A, Hanford LE, Heintz N, Henson PM, Hogaboam C, Kagan VE, Keane MP, Kunkel SL, Land S, Loyd JE, Lukacs N, MacPherson M, Manning B, Manning N, Martinelli M, Moller DR, Morse D, Mossman B, Noble PW, Nowak N, Oury TD, Pardo A, Perez A, Petty TL, Phan SH, Ramos-Nino ME, Ray P, Rogers RM, Sato H, Scapoli L, Schaefer LM, Selman M, Stern M, Strollo DC, Tyurin VA, Valnickova Z, Welsh KI, Witzmann FA, Yousem SA, and Strieter RM. Idiopathic pulmonary fibrosis. *Am J Respir Cell Mol Biol* 29: S1–S105, 2003.
23. Sato N, Suzuki Y, Nishio K, Suzuki K, Naoki K, Takeshita K, Kudo H, Miyao N, Tsumura H, Serizawa H, Suematsu M, and Yamaguchi K. Roles of ICAM-1 for abnormal leukocyte recruitment in the microcirculation of bleomycin-induced fibrotic lung injury. *Am J Respir Crit Care Med* 161: 1681–1688, 2000.
24. Schulman CI, Wright JK, Nwariaku F, Sarosi G, and Turnage RH. The effect of tumor necrosis factor-alpha on microvascular permeability in an isolated, perfused lung. *Shock* 18: 75–81, 2002.
25. Sheppard D. Pulmonary fibrosis: a cellular overreaction or a failure of communication? *J Clin Invest* 107: 1501–1502, 2001.
26. Sime PJ, Xing Z, Graham FL, Csaky KG, and Gauldie J. Adenovector-mediated gene transfer of active transforming growth factor-beta1 induces prolonged severe fibrosis in rat lung. *J Clin Invest* 100: 768–776, 1997.
27. Snider GL, Hayes JA, and Korthy AL. Chronic interstitial pulmonary fibrosis produced in hamsters by endotracheal bleomycin: pathology and stereology. *Am Rev Respir Dis* 117: 1099–1108, 1978.
28. Stratton R, Rajkumar V, Ponticos M, Nichols B, Shiwen X, Black CM, Abraham DJ, and Leask A. Prostacyclin derivatives prevent the fibrotic response to TGF-beta by inhibiting the Ras/MEK/ERK pathway. *FASEB J* 16: 1949–1951, 2002.
29. Stratton R, Shiwen X, Martini G, Holmes A, Leask A, Haberberger T, Martin GR, Black CM, and Abraham D. Iloprost suppresses connective tissue growth factor production in fibroblasts and in the skin of scleroderma patients. *J Clin Invest* 108: 241–250, 2001.
30. Tanouchi T, Kawamura M, Ohyama I, Kajiwara I, Iguchi Y, Okada T, Miyamoto T, Taniguchi K, Hayashi M, Iizuka K, and Nakazawa M. Highly selective inhibitors of thromboxane synthetase. 2 Pyridine derivatives. *J Med Chem* 24: 1149–1155, 1981.
31. Uhal BD, Joshi I, True AL, Mundle S, Raza A, Pardo A, and Selman M. Fibroblasts isolated after fibrotic lung injury induce apoptosis of alveolar epithelial cells in vitro. *Am J Physiol Lung Cell Mol Physiol* 269: L819–L828, 1995.
32. Wang Q, Wang Y, Hyde DM, Gotwals PJ, Koteliansky VE, Ryan ST, and Giri SN. Reduction of bleomycin induced lung fibrosis by transforming growth factor beta soluble receptor in hamsters. *Thorax* 54: 805–812, 1999.
33. Wiles ME, Welbourn R, Goldman G, Hechtman HB, and Shepro D. Thromboxane-induced neutrophil adhesion to pulmonary microvascular and aortic endothelium is regulated by CD18. *Inflammation* 15: 181–199, 1991.

TISSUE ENGINEERING
Volume 12, Number 6, 2006

Technical Report

Assessment of Viability and Osteogenic Ability of Human Mesenchymal Stem Cells After Being Stored in Suspension for Clinical Transplantation

KAORI MURAKI, B.Sc.,[1] MOTOHIRO HIROSE, Ph.D.,[1] NORIKO KOTOBUKI, Ph.D.,[1] YOICHI KATO, B.Sc.,[1] HIROKO MACHIDA, M.Sc.,[1]YOSHINORI TAKAKURA, M.D.,[2] and HAJIME OHGUSHI, M.D.[1]

ABSTRACT

Human mesenchymal stem cells (MSCs) were suspended in phosphate-buffered saline (PBS) and stored up to 24 h at 4°C, 24°C, and 37°C. More than 80% viability was maintained at any temperature for at least 1 h, then gradually decreased over time. After 24 h, the viabilities at 4°C, 24°C, and 37°C were about 81%, 70%, and 62%, respectively. The MSCs suspended/stored in PBS at 4°C for 24 h also exhibited *in vitro* osteogenic differentiation capability as evidenced by mineralized matrix formation as well as high alkaline phosphatase activity when cultured in an osteogenic medium. Furthermore, *in vivo* implantation experiments using the MSCs also demonstrated new bone formation. Because MSCs are known to possess multipotential stem cell characteristics, these data indicate that human MSCs stored in PBS at 4°C could be delivered to distant medical facilities for the purpose of hard tissue and other types of tissue regeneration therapy.

INTRODUCTION

MARROW STROMAL STEM CELLS,[1] recently termed "mesenchymal stem cells (MSCs)"[2] are highly proliferative cells that can be maintained in culture and readily differentiated into mesodermal cell types (fat, bone, cartilage and muscle).[1–3] Many researchers including us have previously reported that human MSCs derived from bone marrow differentiate into osteoblasts by *in vivo* implantation.[4,5] The osteogenic potential of MSCs has already been applied in clinical situations. Horwitz used allogenic MSCs for the treatment of osteogenesis imperfecta,[6] and Quarto *et al.*[7] used autogenous MSCs/ceramic composites for treatments of fractures. The MSCs can also differentiate into osteoblasts by *in vitro* culture with dexamethasone (Dex).[8–10] The *in vitro* differentiation resulted in osteoblastic phenotype expression of MSCs, and the osteoblasts formed extracellular bone matrices with abundant minerals on various culture substrata including ceramic surfaces.[11,12] The *in vitro*-formed osteoblasts/bone matrix on ceramic surface has been used for the treatment of osteoarthritic cases.[13,14] Recent studies have

[1]Tissue Engineering Research Group, Research Institute for Cell Engineering (RICE), National Institute of Advanced Industrial Science and Technology (AIST) Hyogo, Japan.
[2]Department of Orthopedic Surgery, Nara Medical University Nara, Japan.

also shown the possibility that MSCs can differentiate not only into the variety of mesodermal cells, but also into either ectodermal or endodermal cells.[15–20] This ability indicates the usefulness of MSCs for tissue engineering.

As therapies advanced from research laboratories to actual clinical applications, tissue regeneration using MSCs should be considered from practical viewpoints such as the maintenance and transportation of highly functional MSCs. However, optimal storage conditions have not been extensively investigated, especially for MSCs stored in liquid suspension, which could be available as ready-to-use cellular devices.

In this study, we investigated the viability of MSCs suspended in phosphate-buffered saline (PBS) at three different temperatures after storage from 0 to 24 h. We also observed the cell surface antigens and further examined the *in vitro* as well as *in vivo* osteogenic differentiation capability of the MSCs.

MATERIALS AND METHODS

Preparation and culture of marrow cells

Human bone marrow was aspirated from the iliac crest of three donors (16-year-old girl, 26-year-old man, and 29-year-old woman) with informed consent. Three milliliters of the marrow aspirates were immediately collected into a syringe containing 3 mL of PBS (phosphate buffered saline minus Ca^{2+} and Mg^{2+}, Invitrogen Corp., Carlsbad, CA) composed of 0.2 g/L KCl, 0.2 g/L KH_2PO_4, 8.0 g/L NaCl, and 2.16 g/L Na_2HPO_4 and 30 IU of heparin. After centrifugation at 140 ×g for 10 min at 4°C, the supernatants of the plasma and fat layers were discarded. The remaining nucleated cells with the red blood cell layer were seeded/divided into two T-75 flasks (Becton Dickinson Co., NJ) with 15 mL of medium. The culture medium was Eagle's minimum essential medium alpha (α-MEM, Invitrogen Corp.) containing 15% fetal bovine serum (FBS, JRH Biosciences Inc., KS) and antibiotics (100 U/mL penicillin G, 100 μg/mL streptomycin sulfate, and 0.25 μg/mL amphotericin B; Sigma-Aldrich Corp., MO). Primary cultures were maintained in a humidified atmosphere of 5% CO_2 at 37°C. Culture media were renewed two or three times per week. At each medium change, nonadherent red blood cells and hematopoietic cells could be removed. After 10 days, adherent cells became almost confluent.[14]

The adherent cells showed high capability for proliferation and differentiation. Analyses of the cell surface antigens revealed the absence of hematopoietic markers but the presence of mesenchymal cell markers.[21] Therefore, we refer to the cells as mesenchymal stem cells (MSCs) in this article. The cells were released from the substrates using a solution of 0.05 (w/v)% trypsin/0.53 mM EDTA (Invitrogen Corp). The harvested cells were centrifuged to concentrate at a density of 5×10^5 cells/mL in solution for cryopreservation (Cell Banker, Juji Field, Inc., Tokyo, Japan) and frozen at −80°C before use. After thawing, the cryopreserved MSCs attached and proliferated well on the culture dish surface, and their proliferation/differentiation capability was comparable to that of noncryopreserved MSCs.[22]

Cell viability assay

The viability of MSCs was assayed using a NucleoCounter (ChemoMetec, Allerød, Denmark), an instrument for counting mammalian cells, which was equipped with a fluorescence microscope. The cell count system is based on propidium iodide (PI) staining[23] to detect nonviable cells, because the PI only penetrates cells having damaged membranes and binds to DNA. After an additional procedure of complete cell lyses, the PI can bind to DNA in all cells, thus enabling determination of the total number of cells.

After immediate thawing of the frozen MSCs, 5×10^5 of the cells were cultured in a 90-mm^2 tissue culture dish for 7 to 10 days to reach near confluence. After the cells were released by trypsin digestion, the cells at a concentration of 1×10^6 cells/mL were suspended in 600 μL of PBS, and stored for periods from 0 h (immediately used) to 24 h at 4°C, 24°C, and 37°C. To determine viability, 40 μL of each sample diluted five times with PBS was analyzed using the NucleoCounter, giving an estimate of nonviable and total cells.

Although the NucleoCounter provides information of nonviable and total cell number, direct visualization of viable and nonviable cells at the cellular level cannot be

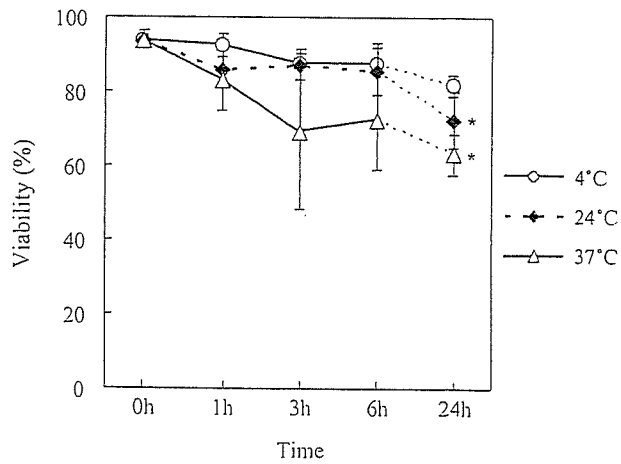

FIG. 1. Percent of viable MSCs stored in PBS at 4°C, 24°C, and 37°C from 0 h to 24 h. The data represent the mean ± SD of the six samples. $*p < 0.05$; significant difference against the viability of the cells stored in PBS at 4°C.

done. To visualize the cells, a LIVE/DEAD Viability Assay Kit (Molecular Probes, Inc., OR) was used to determine the numbers of living and dead cells at the same moment with calcein-AM for intracellular esterase and ethidium homodimer-1(EthD-1) for plasma membrane integrity.

MSCs suspended/stored in PBS at 4°C, 24°C, and 37°C were sampled in the dishes at each time point (0 h, 1 h, 3 h, 6 h, and 24 h), and 2 mM of calcein-AM and 5 mM of EthD-1 in PBS were directly added to the sampled cells at room temperature. After 15 min, the samples were observed by using a fluorescence microscope (IX70, OLYMPUS Co. Ltd., Tokyo, Japan).

Immunostaining and FACS analysis

MSCs suspended/stored in PBS at 4°C, 24°C or 37°C for 24 h were diluted into 1.5-mL centrifuge tubes and incubated with antibodies on ice for 15 min. The cells were pelleted, washed twice in PBS, and analyzed by a FACSCalibur flow cytometer (Becton Dickinson Co.). The antibodies used were CD13-FITC (fluorescein isothiocyanate), CD45-FITC (BIOCARTA Europe, Hamburg, Germany), and CD34-FITC (CARTAG Laboratories, CA).

Osteogenic differentiation assay

MSCs suspended/stored in PBS at 4°C for each time period (0, 1, 3, 6, and 24 h) were seeded at a cell density of 1×10^4 cells/cm^2 in a 12-well culture plate and cultured in media supplemented with 15% FBS, 10 mM β-glycerophosphate (affiliate of Merck KGaA, Darmstadt, Germany), disodium salt, 0.07 mM L-ascorbic acid phosphate (Sigma-Aldrich Corp.), and 0.1 μM dexamethasone (Dex) (Sigma-Aldrich Corp.) for 2 or 3 weeks. Because Dex is known as an osteogenic factor to MSCs,[8,9,21,22] cultures without Dex were used as a negative control. To enable the detection of the mineralized extracellular matrix, 1 μg/mL of calcein (Dojindo Laboratories, Kumamoto, Japan) was added at every media change. After culture for 14 days, the cell layers were washed twice with

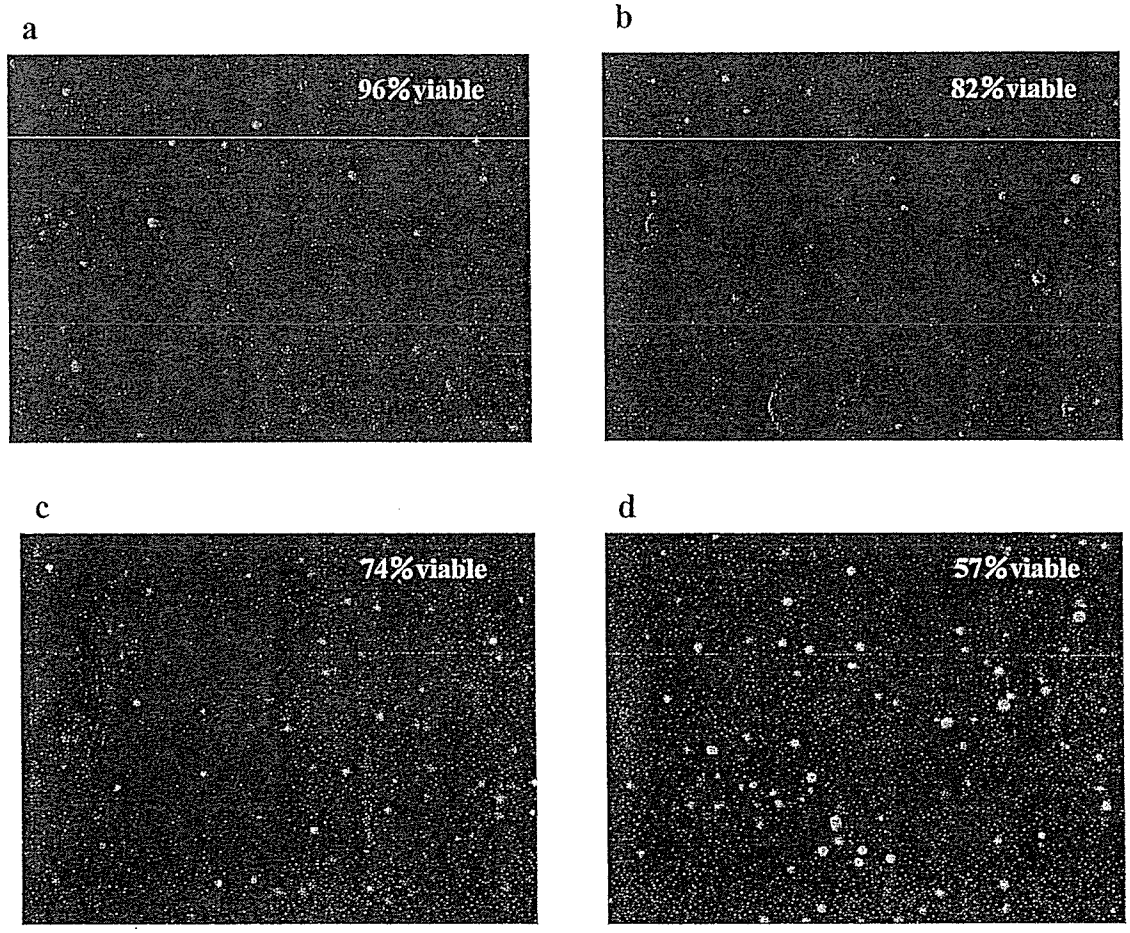

FIG. 2. Fluorescence microscopic view of MSCs stored in PBS after LIVE/DEAD Viability assay. (a) Immediately visualized with no storage, (b) stored at 4°C for 24 h, (c) stored at 24°C for 24 h, and (d) stored at 37°C for 24 h. Green fluorescent signal indicates living cells and red fluorescent signal indicates dead cells.

PBS, and then the fluorescence of the deposited calcein was visualized and quantified by using an image analyzer (Typhoon 8600, Molecular Dynamics, Inc., Sunnyvale, CA).[24] The fluorescent intensities parallel well the contents of calcium in the mineralized matrix.[24] Human fibroblasts (2F0-C25, Cell Systems, CA) were also used as negative controls against MSCs. Human fibroblasts stored at 4°C for 24 h were seeded at a cell density of 1×10^4 cells/cm^2 in a 12-well culture plate and cultured in media comprising 15% FBS, 10 mM β-glycerophosphate, disodium salt, 0.07 mM L-ascorbic acid phosphate, 0.1 μM Dex, and 1 μg/mL calcein. After culture for 21 days, the cell layers were washed twice with PBS, and the fluorescence of the deposited calcein was visualized and quantified by using an image analyzer.

To measure ALP activity, the cell layers from each well were collected into 0.5 mL of 10 mM Tris-buffer (pH 7.4, 1 mM EDTA, 100 mM NaCl) by scraping. The scraped cells were then sonicated and centrifuged at 13,000 ×g for 1 min at 4°C. An aliquot (20 μL) of the supernatant was assayed for ALP (alkaline phosphatase) activity using a *p*-nitrophenyl phosphate substrate (Zymed Laboratories Inc., CA).[9,11] The ALP activity was represented by *p*-nitrophenol, which was released after incubation for 30 min at 37°C. In the case of *in vivo* study, implants as described below were homogenized and sonicated in the above buffer solution prior to the ALP activity assay.

Implantation of MSCs/ HA constructs into athymic nude rats

MSCs suspended/stored in PBS at 4°C for 0 h or 24 h at a cell density of 1×10^6 cells/mL were added to porous hydroxyapatite (HA) disks of 5 mm in diameter (Apaceram, Pentax Corp., Tokyo, Japan) and incubated at 37°C for 3 h. The HA disks were transferred to 24-well Falcon tissue culture dishes and subcultured in media containing 15% FBS, 10 mM β-glycerophosphate, disodium salt, 0.07 mM L-ascorbic acid phosphate, and 0.1 μM Dex for 2 weeks for fabrication of MSCs/HA constructs. Seven-week-old male athymic nude Fischer 344 rats (Fischer 344/N Jcl-rnu, Clea Japan, Inc., Tokyo, Japan) were anesthetized by intramuscular injection of pentobarbital (Nembutal, Dainippon Pharmaceutical Co. Ltd., Osaka, Japan) at a final concentration of 3.5 mg/100 g body weight. Six MSCs/HA constructs and two HA disks without cells were implanted subcutaneously into the back of each athymic nude rat; three constructs fabricated from MSCs stored for 0 h and one HA disk without cells were implanted in the right side, and the other three constructs fabricated from MSCs stored for 24 h and one HA disk without cells were separately implanted in the left side. The recipient rats used were two. HA disks without cells were used as negative controls. Animal experiments were carried out in compliance with Japanese Law (No. 105) on animal protection and administration as well as the Regulation on the Imple-

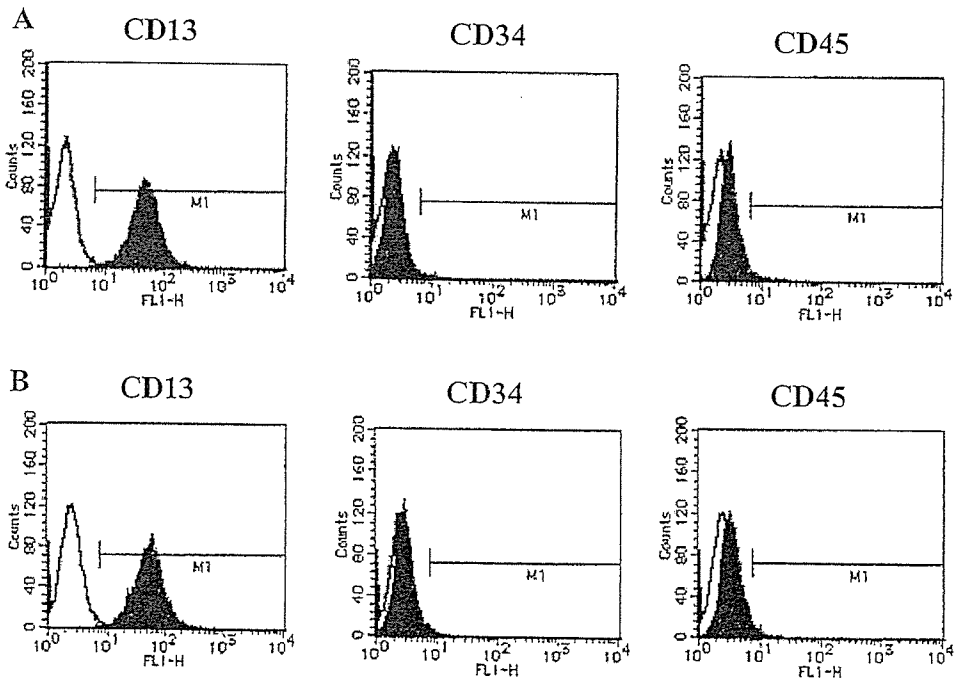

FIG. 3. FACS analysis of MSCs (A) and MSCs stored in PBS at 4°C for 24 h (B). Both cell types were reacted with each CD antibody and then loaded into a flow cytometer. The open histograms show the fluorescence intensity of the cells with negative control IgG. The closed histograms show the fluorescence intensity of the cells with each CD antibody.

mentation of Animal Experimentation of the AIST (Independent Administrative Organization, National Institute of Advanced Industrial Science and Technology).

Analysis of the implants

All implants (MSCs/HA constructs and HA disks without cells) were harvested 6 weeks postimplantation. Each of four constructs fabricated from MSCs stored for 0 h and 24 h, respectively, was used for ALP activity assay as described above. The other constructs and HA disks without cells were fixed with 10% buffered formalin, decalcified with K-CX solution (Falma Co., Tokyo, Japan), and then stained with hematoxylin and eosin. These specimens were examined by light microscopy.

Statistics

All the data were analyzed for statistical significance using Student's *t*-test computed by JMP 5.0 software (SAS Institute, Inc.), and statistical significance was accepted at $p < 0.05$. Experimental results were expressed as the means ± standard deviation (SD) of the mean.

RESULTS

Viability of MSCs suspended/stored in PBS

After culturing MSCs in 90-mm^2 tissue culture dishes for about 10 days, the cells were trypsinized and suspended with PBS at a concentration of 1×10^6 cells/mL and stored at 4°C, 24°C, and 37°C. The viability (percent of total cells that were viable) of the MSCs in the PBS was assayed by a NucleoCounter. The assay was done at different storage intervals (from 0 to 24 h). Cell viability was maintained at more than 80% at any temperature of 4°C, 24°C, and 37°C after 1 h, then gradually decreased over time. The decrease was most apparent for the MSCs stored at 37°C, showing about 61% viability after 24 h. At 4°C and 24°C after 6 h, viabilities were both about 85% and those after 24 h were about 81% and 70%, respectively (Fig. 1). Concerning the cells stored for 24 h, statistical differences are seen among the percent viabilities at 4°C, 24°C, and 37°C.

The viabilities at the single-cell level were visualized by a LIVE/DEAD Viability Assay Kit. As shown in Fig. 2, most cells were green (viable cells) and only a few

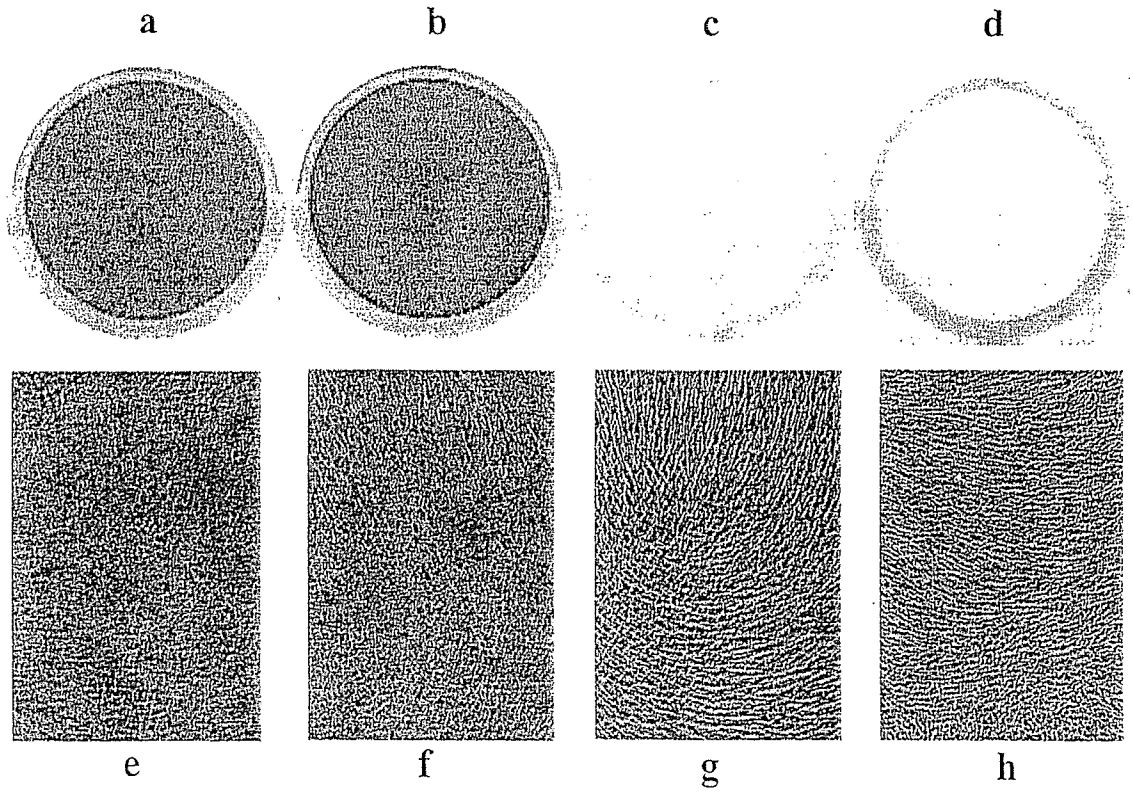

FIG. 4. Mineralization of MSCs on culture dishes. MSCs (a, b, c, e, f, and g) and human fibroblasts (d and h) were cultured in the presence of Dex (a, b, d, e, f, and h) or absence of Dex (c and g) for 21 days in 12-well plates. Culture medium contained glycerophosphate and calcium binding fluorescent dye of calcein. After being washed with PBS, the culture dish was visualized using an image analyzer. Fluorescence uptake (a, b, c, and d) and phase contrast view of culture (e, f, g, and h) are shown. MSCs stored in PBS at 4°C for 0 h (a and e) and 24 h (b, c, f, and g) were used for the culture. Black dots (a and b) indicate calcium deposition by fluorescence intensity. (Color images are available at <www.liebertpub.com/ten>.)

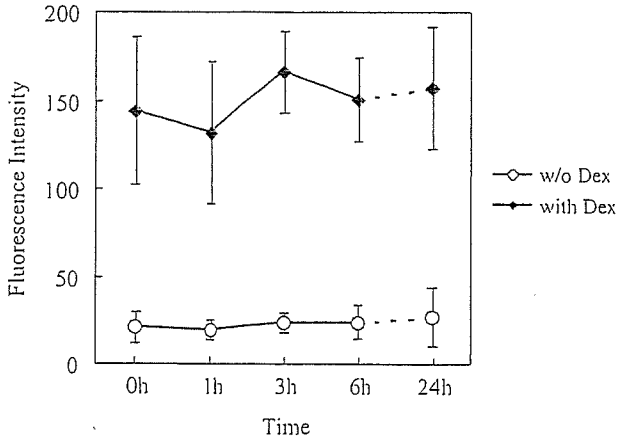

FIG. 5. Fluorescence intensity of cultured MSCs after being stored in PBS at 4°C from 0 h (immediately seeded) to 24 h. The culture occurred in the presence or absence of Dex for 14 days. The data represent the mean ± SD of the six samples.

cells were red (nonviable cells) in cultured MSCs before suspension in PBS. After the MSCs suspension/storage in PBS for 24 h at 4°C, 24°C, and 37°C, the number of green cells decreased, indicating a loss of viability. The percents of green cells (viable) at 4°C, 24°C, and 37°C were 82, 74, and 57, respectively. These data were comparable with those assayed by NucleoCounter (Fig. 1).

Immunostaining and FACS analysis

MSCs suspended/stored in PBS at 4°C after 24 h were analyzed by a flow cytometer for the expressions of CD13, CD34, and CD45 surface antigens and were compared with these expressions of MSCs without storage. Representative results are shown in Fig. 3. Both MSC samples showed similar patterns, that is, cells from both samples were not positive for the expression of hematopoietic markers of CD34 and 45, but strongly positive for CD13 (Aminopeptidase N), which is known to be present in MSCs.[25]

MSCs suspended/stored in PBS at 24°C and 37°C for 24 h also showed similar expression patterns (data are not shown). These results showed that the cell surface expression patterns had not been changed after being suspended/stored for 24 h. Only living cells were gated and analyzed.

Differentiation assay

MSCs suspended/stored in PBS at 4°C for 0 h (immediately used) to 24 h were seeded on a 12-well culture plate and cultured in osteogenic medium. The medium contained β-glycerophosphate, L-ascorbic acid 2-phosphate and, importantly, Dex, which is known to induce undifferentiated MSCs into osteoblasts,[8,21,22] resulting in the formation of a mineralized matrix. As we previously reported, the mineralization (bone matrix formation) could be detected after about 10 to 14 days of culture and more obviously after 21 days.[8,21] As shown in Fig. 4, the culture with Dex for 21 days showed mineralization (amorphous brown color in Fig. 4e and f), which was confirmed by calcein uptake (black areas in Fig. 4a and b). After storage in PBS, the mineralization capacity of MSCs (Fig. 4b and f) was comparable to that without storage (Fig. 4a and e). In contrast, the culture without Dex showed no mineralization (Fig. 4c and g).

Because fibroblasts never exhibit mineralization even culturing with Dex,[24] we also cultured human fibroblasts in the presence Dex as negative controls of differentiation assays. As shown in Fig. 4d and g, human fibroblasts stored at 4°C for 24 h before culture did not show mineralization. These qualitative results indicate that storage at 4°C for 24 h does not affect the osteoblastic differentiation capability of MSCs.

To demonstrate quantitative data, we measured the amount of mineralization and ALP activity, which localizes at the cell membranes of osteoblasts.[26] As shown in Fig. 5, the amounts of mineralization detected by fluorescent uptake of calcein were much higher for the culture in the presence of Dex compared with the culture in the absence of Dex. The high uptake was seen by culturing MSCs suspended/stored in PBS for 0 h to 24 h. The data coincided well with the data of ALP (Fig. 6), which also demonstrated the high ALP activity of MSCs cultured in the presence of Dex. The high level was also detected by culturing MSCs suspended/stored in PBS for 0 to 24 h. As shown in the results, MSCs maintained a high level of osteogenic ability *in vitro* after storage at 4°C for 24 h.

Next, we addressed the *in vivo* ability of MSCs after storage. We have previously reported that MSCs/HA con-

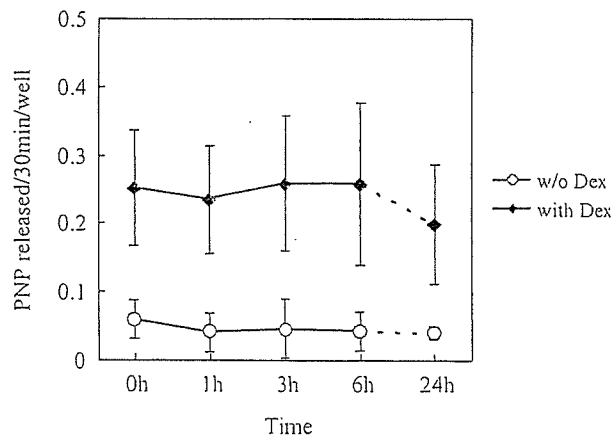

FIG. 6. ALP activity of cultured MSCs after being stored in PBS at 4°C from 0 h (immediately seeded) to 24 h. The culture occurred in the presence or absence of Dex for 14 days. The data represent the mean ± SD of the six samples (*p*-nitrophenol release/30 min/well).

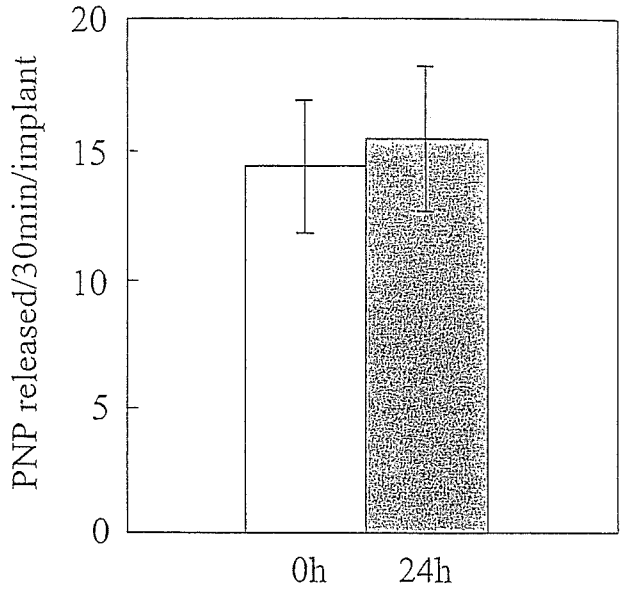

FIG. 7. ALP activity of MSCs/HA constructs after 6-week implantation. MSCs stored at 4°C for 0 h (open bar) or 24 h (closed bar) were cultured on HA disks with Dex for 2 weeks. The MSCs/HA constructs were implanted into athymic nude rats. After 6-week implantation, ALP activity of the constructs was measured. The data represent the mean ± SD of four samples (*p*-nitrophenol released/30 min/implant). (Color images are available at <www.liebertpub.com/ten>.)

structs treated with Dex could show a high level of osteogenic ability after *in vivo* implantation.[27] According to the methods, we prepared the constructs fabricated from MSCs stored at 4°C for 0 h or for 24 h and also HA disks without cells as negative controls, then implanted at subcutaneous sites of athymic nude rats. After 6-week implantation, both constructs showed similar high ALP activity (Fig. 7). Histologic appearance also demonstrated that both constructs showed newly formed bone with active osteoblasts (Fig. 8). However, implants of HA disks without cells did not show any bone formation (Fig. 8).

From these results, we concluded that MSCs suspended/stored in PBS at 4°C up to 24 h could maintain a high level of viability and capability of differentiation *in vitro* as well as *in vivo*.

DISCUSSION

Mesenchymal stem cells (MSCs) can differentiate into osteogenic lineage, and the osteogenic potential of MSCs has already been applied in clinical situations.[6,7,14] Recent studies have also demonstrated the possibility that MSCs can differentiate into other types of tissue-specific cells such as cardiac myoblasts,[15,16] vascular endothelial cells,[17,18] hepatocytes,[19] and neural cells.[20] These results indicate the usefulness of multipotential MSCs for a wide range of tissue engineering purposes in regenerative medicine. In considering the clinical applications of MSCs, the number of MSCs in bone marrow is extremely low,[2,13] and thus a procedure for culture expansion of MSCs is needed. However, such procedures introduce risks for bacterial/fungal contamination. To avoid these risks, biologically safe areas such as a cell processing center (CPC) having clean rooms and careful/safe handling are required. However, it is difficult to provide these facilities in many hospitals, primarily because of limited finances. Therefore, there has been an attempt to establish CPCs, which are available upon request by hospitals. This situation requires delivery of the cultured MSCs from the CPC to the hospital in need. The MSCs must be stored in optimal conditions that guarantee their viability as well as differentiation capability for a specific period.

When hematopoietic cells are stored in suspension, a temperature of around 4°C is recommended to maintain cell viability and function.[28] However, there is no simi-

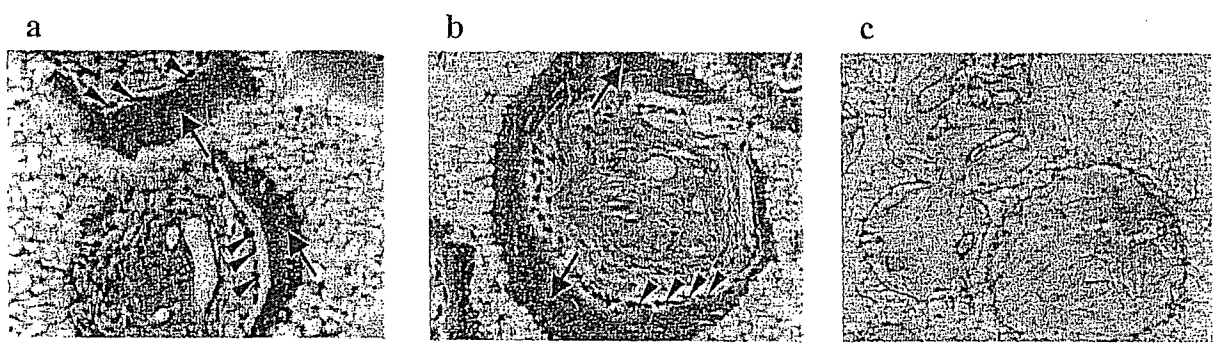

FIG. 8. Histological appearance of MSCs/HA constructs after 6-week implantation. MSCs stored at 4°C for 0 h (a) or 24 h (b) were cultured on HA disks with Dex for 2 weeks. The MSCs/HA constructs were implanted into athymic nude rats. After 6-week implantation, the constructs were decalcified and stained with hematoxylin and eosin. HA disks without MSCs were implanted as negative controls (c). The light microscopy was performed. Arrows show bone matrices in porous areas of HA. Arrowheads show the bone forming active osteoblasts. Original magnification ×200.

lar information about the optimal temperature and conditions for maintaining the viability of adherent cell MSCs. This study focused on investigating viability assessment for successful transportation of MSCs in suspension based on three major factors: incubation time, type of storage medium, and temperature. We also examined osteogenic differentiation capability of MSCs stored in suspension.

Our preliminary data showed that there was no difference of MSC viability in the three kinds of media, PBS, saline, and α-MEM (data not shown). Among them, the composition of PBS and saline are simpler than that of α-MEM. Saline may cause pH changes because there is no buffering action. For these reasons, in the present study we selected PBS as the storage medium for MSCs.

As shown in Fig. 1, MSCs maintained more than 85% viability at both 4°C and 24°C for 6 h, and more than 80% viability at 4°C for 24 h, whereas the viability of the cells stored at 24°C and 37°C for 24 h was significantly decreased. Because the viability at 4°C was most acceptable and it is relatively easy to regulate/maintain the temperature at 4°C, we further performed osteogenic differentiation assay *in vitro* as well as *in vivo* using the cell stored at 4°C. The MSCs suspended/stored in PBS at 4°C for 24 h did not lose their capability for *in vitro* osteogenic differentiation. This is confirmed by the high degree of mineralization and ALP activity of the MSCs after culturing in the presence of Dex (Figs. 4–6). Importantly, the mineralization and ALP activities were comparable to those of control MSCs (nonstored MSCs). The expression of cell surface antigen patterns was similar for the MSCs stored for 24 h and the control MSCs. Consistent with the *in vitro* findings, *in vivo* implants of MSCs/HA construct demonstrated high ALP activity and bone-forming capability using MSCs after the storage. These results thus demonstrated that MSCs can maintain cell viability and osteogenic capability even after 24 h when stored in PBS at 4°C. These conditions enable the delivery of MSCs to distant medical facilities without serious loss of MSC function for the various purposes of tissue regeneration, especially hard tissue regeneration.

The present data clearly showed the durability of MSCs suspended/stored in PBS and that MSCs can be available not only locally but also in distant areas without significant loss of viability as well as differentiation (especially osteogenic differentiation) capability. Therefore, this process represents an opportunity for developing new therapeutic strategies using MSCs.

ACKNOWLEDGMENTS

We thank our colleagues at the National Institute of Advanced Industrial Science and Technology (AIST) and at Nara Medical University. This work was supported by the Three-Dimensional Tissue Module Project of METI (a Millennium Project) and a Grant-in-Aid for Scientific Research.

REFERENCES

1. Owen, M. Marrow stromal stem cells. J. Cell. Sci. Suppl. **10**, 63, 1988.
2. Caplan, A.I. Mesenchymal stem cells. J. Orthop. Res. **9**, 641, 1991.
3. Pittenger, M.F., Mackay, A.M., Beck, S.C., Jaiswal, R.K., Douglas, R., Mosca, J.D., Moorman, M.A., Simonetti, D.W., Craig, S., and Marshak, D.R. Multilineage potential of adult human mesenchymal stem cells. Science **284**, 143, 1999.
4. Ohgushi, H., and Okumura, M. Osteogenic capacity of rat and human marrow cells in porous ceramics. Acta Orthop. Scand. **61**, 431, 1990.
5. Caplan, A.I., and Bruder, S.P. Mesenchymal stem cells: Building blocks for molecular medicine in the 21st century. Trends Mol. Med. **259**, 7, 2001.
6. Horwitz, E.M., Gordon, P.L., Koo, W.K., Marx, J.C., Neel, M.D., McNall, R.Y., Muul, L., and Hofmann, T. Isolated allogeneic bone marrow-derived mesenchymal cells engraft and stimulate growth in children with osteogenesis imperfecta: Implications for cell therapy of bone. Proc. Natl. Acad. Sci. U S A **99**, 8932, 2002.
7. Quarto, R., Mastrogiacomo, M., Cancedda, R., Kutepov, S. M., Mukhachev, V., Lavroukov, A., Kon, E., and Marcacci, M. Repair of large bone defects with the use of autologous bone marrow stromal cells. N. Engl. J. Med. **344**, 385, 2001.
8. Maniatopoulos, C., Sodek, J., and Melcher, A.H. Bone formation *in vitro* by stromal cells obtained from bone marrow of young adult rat. Cell Tissue Res. **254**, 317, 1988.
9. Ohgushi, H., Dohi, Y., Katuda, T., Tamai, S., Tabata, S., and Suwa, Y. *In vitro* bone formation by rat marrow cell culture. J. Biomed. Mater. Res. **32**, 333, 1996.
10. Bruder, S.P., Jaiswal, N., and Haynesworth, S.E. Growth kinetics, self-renewal, and the osteogenic potential of purified human mesenchymal stem cells during extensive subcultivation and following cryopreservation. J. Cell Biochem. **64**, 278, 1997.
11. Ohgushi, H., Yoshikawa, T., Nakajima, H., Tamai, S., Dohi, Y., and Okunaga, K. Al_2O_3 doped apatite-wollastonite containing glass ceramic provokes osteogenic differentiation of marrow stromal stem cells. J. Biomed. Mater. Res. **44**, 381, 1999.
12. Kitamura, S., Ohgushi, H., Hirose, M., Funaoka, H., Takakura, Y., and Ito, H. Osteogenic differentiation of human bone marrow-derived mesenchymal cells cultured on alumina ceramics. Artif. Organs **28**, 72, 2004.
13. Ohgushi, H., and Caplan, A.I. Stem cell technology and bioceramics: From cell to gene engineering. J. Biomed. Mater. Res. **48**, 913, 1999.
14. Ohgushi, H., Kotobuki, N., Funaoka, H., Machida, H., Hirose, M., Tanaka, Y., and Takakura, Y. Tissue engineered ceramic artificial joint: *Ex vivo* osteogenic differentiation of patient mesenchymal cells on total ankle joints for treatment of osteoarthritis. Biomaterials **26**, 4654, 2005.

15. Makino, S., Fukuda, K., Miyoshi, S., Konisho, F., Kodama, H., Pan, J., Sano, M., Takahashi, T., Hori, S., Abe, H., Hata, J., Umezawa, A., and Ogawa, S. Cardiomyocytes can be generated from marrow stromal cells *in vitro*. J. Clin. Invest. **103**, 697, 1999.
16. Nagaya, N., Fujii, T., Iwase, T., Ohgushi, H., Itoh, T., Uematsu, M., Yamagishi, M., Mori, H., Kangawa, K., and Kitamura, S. Intravenous administration of mesenchymal stem cells improves cardiac function in rats with acute myocardial infarction through angiogenesis and myogenesis. Am. J. Physiol. Heart Circ. Physiol. **287**, H2670, 2004.
17. Reyes, M., Dudek, A., Jahagirdar, B., Koodie, L., Marker, P.H., and Verfaillie, C.M. Origin of endothelial progenitors in human postnatal bone marrow. J. Clin. Invest. **109**, 337, 2002.
18. Akahane, M., Ohgushi, H., Kuriyama, S., Akahane, T., and Takakura, Y. Hydroxyapatite ceramics as a carrier of gene-transduced bone marrow cells. J. Orthop. Sci. **7**, 677, 2002.
19. Schwartz, R.E., Reyes, M., Koodie, L., Jiang, Y., Blackstad, M., Lund, T., Lenvik, T., Johnson, S., Hu, W.S., and Verfaillie, C.M. Multipotent adult progenitor cells from bone marrow differentiate into functional hepatocyte-like cells. J. Clin. Invest. **109**, 1291, 2002.
20. Deng, W., Obrocka, M., Fischer, I., and Prockop, D.J. *In vitro* differentiation of human marrow stromal cells into early progenitors of neural cells by conditions that increase intracellular cyclic AMP. Biochem. Biophys. Res. Commun. **282**, 48, 2000.
21. Kotobuki, N., Hirose, M., Takakura, Y., and Ohgushi, H. Cultured autologous human cells for hard tissue regeneration: Preparation and characterization of mesenchymal stem cells from bone marrow. Artif. Organs **28**, 33, 2004.
22. Kotobuki, N., Hirose, M., Machida, H., Katou, Y., Muraki, K., Takakura, Y., and Ohgushi, H. Viability and osteogenic potential of cryopreserved human bone marrow derived mesenchymal cells. Tissue Eng. **11**, 663, 2005.
23. Jones, K. H., and Senft, J. A. An improved method to determine cell viability by simultaneous staining with fluorescein diacetate-propidium iodide. J. Histochem. Cytochem. **33**, 77, 1985.
24. Uchimura, E., Machida, H., Kotobuki, N., Kihara, T., Kitamura, S., Ikeuchi, M., Hirose, M., Miyake, J., and Ohgushi, H. *In-situ* visualization and quantification of mineralization of cultured osteogenetic cells. Calcif. Tissue Int. **73**, 575, 2003.
25. Pittenger, M.F., and Martin, B.J. Mesenchymal stem cells and their potential as cardiac therapeutics. Circulation Res. **95**, 9, 2004.
26. Stewart, K., Walsh, S., Screen, J., Jefferiss, C.M., Chainey, J., Jordan, G.R., and Beresford, J.N. Further characterization of cells expressing STRO-1 in cultures of adult human bone marrow stromal cells. J. Bone Miner. Res. **14**, 1345, 1999.
27. Ohgushi, H., Goldberg, V.M., and Caplan, A.I. Heterotopic osteogenesis in porous ceramics induced by marrow cells. J. Orthop. Res. **7**, 568, 1989.
28. Lasky, L.C., McCullough, J., and Zanjani, E.D. Liquid storage of unseparated human bone marrow. Evaluation of hematopoietic progenitors by clonal assay. Transfusion **26**, 331, 1986.

Address reprint requests to:
Motohiro Hirose, Ph.D.
Tissue Engineering Research Group
Research Institute for Cell Engineering (RICE)
National Institute of Advanced Industrial Science and Technology (AIST)
Nakoji 3-11-46, Amagasaki, Hyogo 661-0974, Japan

E-mail: motohiro-hirose@aist.go.jp

動脈疾患　閉塞性動脈硬化症

竹下　聡*
たけした　さとし

● 閉塞性動脈硬化症は quality of life への影響は大きいが，生命予後に対する影響は小さい．
● 閉塞性動脈硬化症患者の生命予後は，合併する動脈硬化性疾患によって規定される．
● 閉塞性動脈硬化症の早期発見によって，動脈硬化の危険因子コントロールを早期に開始し，虚血性心疾患や脳血管疾患の予防へと結びつけることが肝要である．

Key Words：ABPI，Fontaine 分類，血管超音波検査，近赤外線分光法

はじめに

人は血管とともに老いると言われるように，動脈硬化は加齢とともに進行する．この進行に影響を与えるのが，糖尿病，高脂血症，高血圧，喫煙などの動脈硬化性危険因子である．これらの危険因子を治療することによって，狭心症や心筋梗塞などの動脈硬化性疾患の進行を阻止することが可能である．これは閉塞性動脈硬化症においても同様で，より早期に発見し危険因子のコントロールを開始することが患者予後の改善において肝要である．

閉塞性動脈硬化症とは

従来，閉塞性動脈硬化症はわが国では少なく，同じ末梢動脈閉塞疾患である Buerger 病が多数を占めるとされていた．しかしながら，食生活の欧米化とともに閉塞性動脈硬化症が増加し，Buerger 病の占める割合は次第に減少してきた．

わが国における閉塞性動脈硬化症の発生頻度については，大規模な疫学データが存在しないため詳細は不明であるが，欧米における罹患率は人口の数パーセント程度とされている[1]．

閉塞性動脈硬化症では，末梢動脈の粥状動脈硬化によって血管内腔の狭窄が進行し，下肢虚血が生じる．これにともない，しびれ，冷感，間歇性跛行，疼痛，潰瘍，壊疽などのさまざまな症状が出現する．自覚症状による病期分類としては Fontaine 分類が代表的である（表 1）．Fontaine

表 1　Fontaine 分類

グレード	症　状
I	無症状
II	間歇性跛行
III	安静時疼痛
IV	皮膚潰瘍，壊疽

I 度の軽症（無症状）患者に対しては，禁煙指導を行ったり，糖尿病・高血圧など動脈硬化の危険因子コントロールを行いながら経過を観察する．病状が進行してくると，Fontaine II度に見られるような間歇性跛行が出現する．間歇性跛行とは，一定距離の歩行後に下肢の疼痛が出現するが，休息により痛みは一時的に消失し，再び歩行することによって再出現するといった特徴的な症状をいう．閉塞性動脈硬化症でもっとも多い症状は，この間歇性跛行である．間歇性跛行が軽度の場合，運動療法や抗血小板剤などによる薬物療法を行うが，重症例では狭窄した血管をカテーテルによって拡張する経皮的血管形成術（percutaneous transluminal angioplasty：PTA）や外科手術（バイパス手術）による血行再建が必要となる．Fontaine III～IV度を重症下肢虚血（critical limb ischemia：CLI）と呼ぶ．このような状態にまで進行すると，安静時にも下肢疼痛が出現し，皮膚潰瘍や壊疽も見られるようになる．重症下肢虚血を呈する患者では，痛みや壊疽のために運動療法を施行するのは困難で，薬物治療に対する反応性も

* 国立循環器病センター　心臓血管内科

0913-7963/06/¥500/論文/JCLS

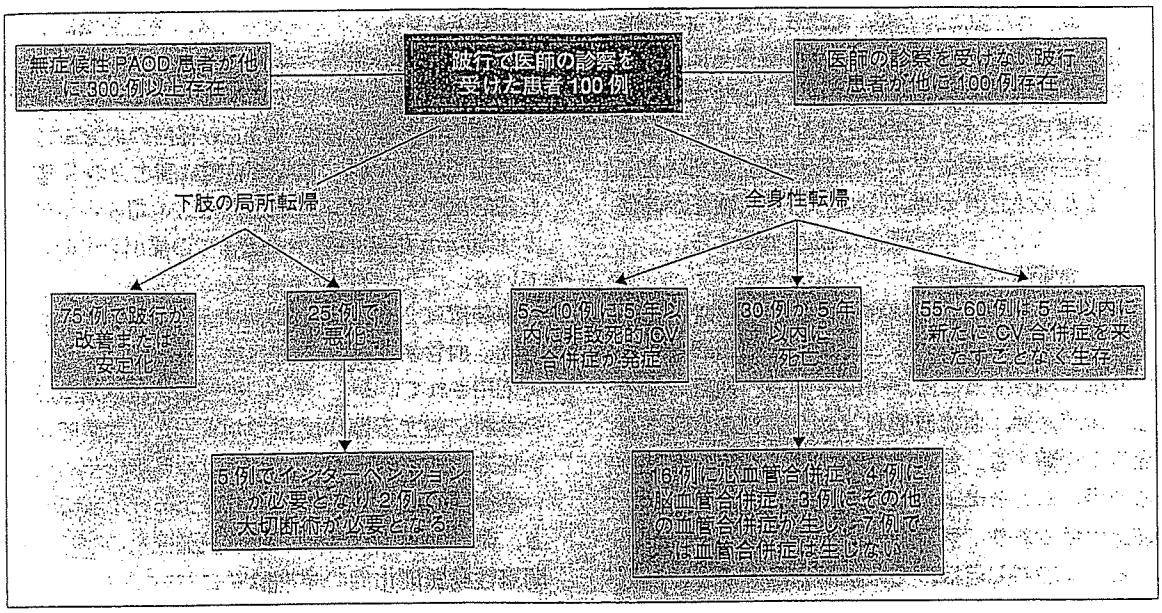

図1　跛行患者の5年間の経過

（文献1日本語訳：日本脈管学会編：下肢閉塞性動脈硬化症の診断・治療指針　日本語版，p. 21，2000より引用）

低い．また，重症下肢虚血をきたすような血管は動脈硬化が高度で，血管形成術やバイパス手術の適応にならないことも少なくない．このような重症例に対しては血管新生療法（therapeutic angiogenesis[2]）が考慮されることになる．

□ 閉塞性動脈硬化症の早期発見

動脈硬化を原因とする疾患として，閉塞性動脈硬化症以外に心筋梗塞などの冠動脈疾患，脳梗塞などの脳血管疾患などさまざまな循環器疾患があげられる．心筋梗塞や脳梗塞が生命に関わるような重篤な疾患であるのに対し，閉塞性動脈硬化症は主にquality of lifeへ関与するため，その早期発見に対する医療従事者の関心は，冠動脈疾患などのそれに比べて低い．

閉塞性動脈硬化症の大部分は，Fontaine II度の間歇性跛行患者で占められる．Fontaine II度の閉塞性動脈硬化症が進行し，下肢血管に対する血行再建術や下肢切断術が必要となってくる確率は5年間で10%以下である．一方，これらの患者が，冠動脈疾患や脳血管疾患で死亡する確率は20%以上ときわめて高い（図1）[1]．すなわち，閉塞性動脈硬化症患者の早期発見は，閉塞性動脈硬化症の進展阻止よりも，むしろ他の心血管合併症を阻止する意味において重要である．また，Fontaine I度の無症状患者は，間歇性跛行例の3倍以上存在し（図1）[1]，潜在する無症候症患者をいかに見つけるか大きな課題といえる．

▣ Vascular Lab

バスキュラーラボ（vascular lab：血管検査室）は，血管疾患の診断を行うためのさまざまな無侵襲検査装置を集約した検査室である．診断装置には四肢血圧脈波測定装置，末梢血管診断装置（バソガード），超音波診断装置，近赤外分光法，トレッドミルなどがある．DSAやCT-angiographyなどの診断法との大きな違いは，血管疾患の画像診断だけでなく，血管の機能評価も行える点にある．

1．上腕・足関節血圧比（ABPI）

上腕・足関節血圧比（ankle-brachial pressure index：ABPI）は，上肢と下肢の収縮期血圧の比から末梢動脈病変の有無を推定する基本指標である．四肢血圧脈波測定装置，末梢血管診断装置（バソガード），ドプラ血流計などを用いて測定する．上肢収縮期血圧は上腕動脈または橈骨動脈で，下肢収縮期血圧は足背動脈または後頸骨動脈で求め，下肢血圧の上肢血圧に対する比を算出する．

0.9未満を異常値とするが，ABPIの低下は早期より認められるため，無症状例の早期発見に有用である．閉塞性動脈硬化症に対するABPIの診断感度と特異度はともに90%を超えるとされているが，慢性透析症例などでは血管が高度に石灰化しているためABPIが低下しない（下肢血圧が高値となる）ので，その評価には注意を要する．

2．血管超音波検査

血管超音波検査は末梢動脈疾患の早期診断にもっとも有用な検査の1つである．無侵襲なので繰り返し施行することが可能である．血管の断層像，血流速度，血流波形などから病変の有無や重症度を判断する．最近の機器では，カラードプラ法を用いることによって，きわめて良好に血流を描出可能であり，病変の検出率向上につながっている．本法の欠点は，その診断精度が術者の技量に大きく依存する点にある．術者の育成に加え，学会などによる検査法の標準化が急務といえる．

3．近赤外線分光法

近赤外線分光法（near infrated spectroscopy：NIRS）は，酸化ヘモグロビンと還元ヘモグロビンの相対変化を測定することで虚血の有無を判定する検査法である．下肢の任意の部位における虚血判定が可能であること，トレッドミルによる歩行負荷時の虚血判定や，負荷後における虚血からの回復過程を経時的に観察可能なことなどが特徴である．たとえば，前述したABPIは閉塞性動脈硬化症に対して優れた診断感度と特異度とを有する．しかしながら，安静時に下肢の血圧低下を呈さないような軽度狭窄病変例や，石灰化の高度な慢性透析例などでの診断には無効なことがある．NIRSは，歩行負荷などを加えることによって軽症例の診断に有用であり，また，マンシェットを必要としないため，高度石灰化例に対する診断にも有用である．

□ 微小血管造影法の早期発見への応用

新エネルギー産業技術総合開発機構（NEDO）の支援のもと，浜松ホトニクス（株）を中心に，NHKエンジニアリングサービス，国立循環器病センター研究所，東海大学医学部などが協力して，病院設置型の微小血管造影装置を開発した．通常の血管造影装置は直径200 μm程度の血管までしか描出できないが，本造影装置は高出力のX線源と高感度のハイビジョン撮像系との組み合わせにより50 μm程度の微小血管までの描出を可能としている．

本装置は2004年に国立循環器病センターに移設され，血管新生療法の施行患者を対象にすでに臨床応用されている[3]．また，糖尿病性微小循環障害の診断に対する臨床応用も始まった．本装置は近い将来，微小血管レベルにおける動脈硬化の新しい画像診断法として用いられる可能性を秘めている．微小血管レベルにおける動脈硬化の進行が，閉塞性動脈硬化症の早期診断においてどのような意味を持つのかは，今後の検討課題である．

おわりに

閉塞性動脈硬化症はquality of lifeへの影響は大きいものの，生命予後に対する影響は小さい．その生命予後は，合併する動脈硬化性疾患によって規定されていると言ってよい．閉塞性動脈硬化症の早期発見によって，動脈硬化の危険因子コントロールを早期に行い，虚血性心疾患や脳血管疾患の予防へと結びつけることが肝要である．

文　献

1）Dormandy JA, Rutherford RB：Management of peripheral artery disease (PAD). TASC Workig Group. J Vasc Surg 31：S 1, 2000

2）Takeshita S, Zheng LP, Brogi E, et al：Therapeutic angiogenesis：a single intraarterial bolus of vascular endothelial growth factor augments revascularization in a rabbit ischemic hind limb model. J Clin Invest 93：662-670, 1994

3）知久正明，ed：微小血管の描出．メディカ出版，大阪，2005．松尾　汎，ed：Vascular Lab増刊　血管検査マニュアル

特　集
循環器疾患の
画像診断
up to date

モダリティの進歩と話題の検査法

微小血管造影
—新生血管描出への応用—

国立循環器病センター心臓血管内科医長　竹下　聡
Takeshita, Satoshi

日本大学医学部附属板橋病院循環器内科　知久　正明
Chiku, Masaaki

Microangiography-visualization of collaterol deveropment-

KEY WORDS

微小血管造影／血管新生

主な略語

DSA：
digital subtraction angiography

CARDIAC PRACTICE
VOL.17 NO.4

はじめに

従来型の血管造影装置の解像度は200～300μmにしかすぎず，これを用いて血管新生療法後の新生血管を描出するのは困難である。なぜなら，血管新生療法により新生する血管は直径100μm以下の微小血管が主体であると考えられるからである[1)-3)]。放射光を用いた微小血管造影により，直径20～50μm前後の微小血管を描出可能であるが，放射光を発生させるには巨大な放射光施設が必要である。たとえば，播磨科学公園都市（兵庫県）にあるSPring 8の周長は1,436mであり，放射光を用いた微小血管造影装置を病院に設置することは現実問題として不可能なのである[1)]。

そこで，われわれは病院設置型微小血管造影装置を開発した。本稿では，この新しい造影法について概説する。

微小血管造影装置の概要

従来，血管新生療法後の微細な血管網の発達を評価するには，digital subtraction angiography（DSA）が用いられてきたが[4)]，その解像度は200μm程度とされており，100μm以下の微小血管を描出することは困難である。

血管新生療法後の微細な血管網の変

■ 従来の血管造影では直径100μm以下の微小血管の描出は困難である。

化を描出するには，微小血管に含まれるわずかな造影剤を検出する必要があり，X線が高輝度で，平行かつ単色であること，また，検出系は高感度・高解像度であることが必須条件となる。血管造影によって描出される血管像とは，血管壁と造影剤との吸収係数の差分が写真用フィルム面に投影されたものである。しかし，X線の一部は人体組織に吸収・減衰されるため，検出系前面における単位面積あたりのX線光子量が減少すると撮影像が劣化する。十分にコントラストのある画像を得るには高輝度のX線が必要となる。放射光施設のX線は一般撮影のX線発生装置の100倍以上の高輝度で，一部が被写体に吸収されても検出系には十分なフォトン数を残すことが可能である。しかしながら，このエネルギー量をもつX線を作ることは一般施設では不可能である。そこでわれわれは，病院設置型微小血管造影装置のX線源として，大容量・大出力を有するCT用X線管を改変して用いることとした。

血管造影にはヨード含有造影剤が使用されるのが一般的であるが，ヨードは33.3 KeVのエネルギーレベルでK吸収端と呼ばれる質量吸収係数が不連続に上昇する性質がある。X線のエネルギーをヨードのK吸収端の直上のエネルギー付近に単色化すると，ヨードと周囲組織との質量吸収係数の差が最大となるので，コントラストの高い画像を得ることができる。実際には金属フィルターを用いて疑似単色化することにより，33.3 KeV(ヨードのK吸収端)前後に10 KeVのバンド幅をもつ擬似単色X線を得ることが可能となる。

病院設置型微小血管造影装置の撮像系は高解像度・高感度の蛍光板(浜松ホトニクス製)と，超高感度・高精細撮像管であるアバランシェ型ハイビジョンカメラ(NHK製)により成り立っている。蛍光板の役割は，X線透亮像を可視光線に変換しグリーン光を発することにある。われわれが用いた蛍光板は蛍光体のみを堆積して作製してあるため，膜厚が薄く光の拡散が小さいという特徴を有する。これは一般の蛍光板に比べ，高解像度化が可能という利点につながる。また，不純物を含まない高密度と微細な柱状結晶構造は減光を大幅に削減し，高感度を保つことが可能となる[5)-8)]。撮像管の光伝導膜はアバランシェ効果により信号増倍を定常状態の600倍まで増倍可能であり，さらに，増倍に伴う雑音が付加されないという特徴も有している。

テストチャートを用いた解像度の検討では，既存の血管造影装置が250μmであったのに対し，微小血管造影装置では50μmと高解像度が実現できた。イヌの冠微小血管の描出に関する実験では，既存の血管造影装置を用いると血管端が不明瞭で，分岐に伴う血管径の減少を確認できなかったが，微小血管造影装置を用いると，心筋貫通枝の血管径が分岐のたびに減じていく様子が詳細に観察可能であった。ウサギの下肢虚血モデルを用いた実験では，既存の血管造影装置では小血管の描出が不良であったのに対し，微小血管造影装置ではアデノシン投与後に100μm以下の微小血管が拡張する様子が鮮明に観察可能であった(図1)。

微小血管造影装置の安全性に関しては，管電圧70kV，管電流500mAで20秒照射した場合，吸収線量は0.547Sv(62.7R)，散乱X線量は0.0225mSv(2.58mR)であり，通常の造影装置と同等の被曝安全性が期待された。

微小血管造影装置の臨床応用

当施設における微小血管造影装置の臨床応用は，血管新生療法の施行症例に限定しており，これまでに計4名に対し合計8回の微小血管造影を施行した。

微小血管造影装置により，100μm以下の微小血管を鮮明に描出することが可能となり，通常のDSAと比較すると，少なくとも1～2分枝以上の末梢側血管が描出可能であった(図2)。1ヵ月～1年の間隔をおいて施行したフォローアップ造影における微小血管の再現性は良好であった。なお，1回の検査における吸収線量は24mGryと臨床上問題のない線量であった。

以上のように，微小血管造影装置は従来の血管造影と同等の安全性を有し

■ *病院設置型微小血管造影装置は直径50μmの微小血管の描出が可能である。*

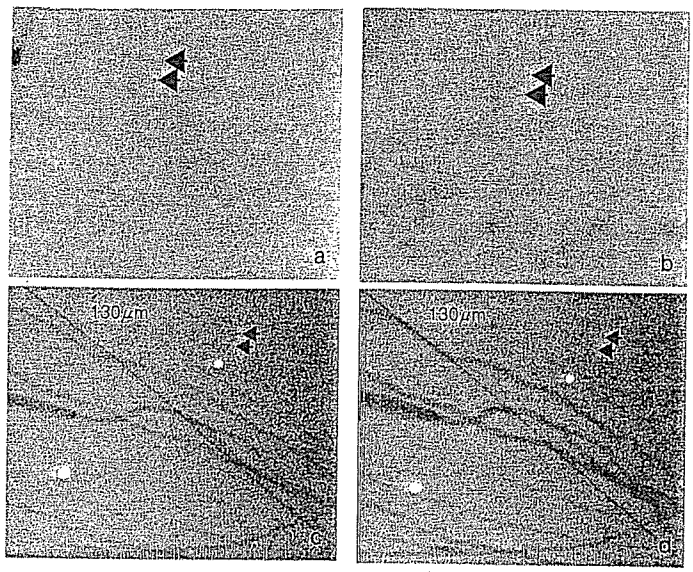

図1　従来の血管造影法と微小血管造影法による家兎の下肢側副血行路の比較

従来法では，アデノシン投与前(a)と投与後(b)のいずれでも側副路の描出は不可能である。しかし，微小血管造影法では側副路が明瞭に描出され，アデノシン投与後(d)では投与前(c)に比べ著明な拡張が認められる。

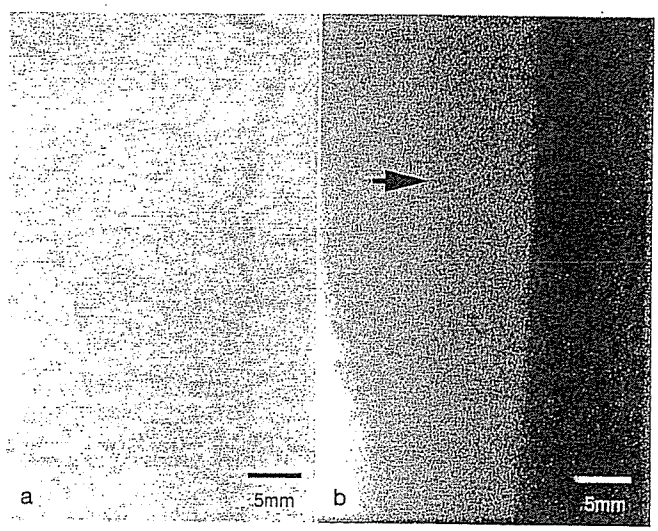

図2　バージャー病症例での微小血管造影

従来法によるDSAでは下肢血管はほとんど描出されないが(a)，微小血管造影法を用いると，そのような領域にも血管が存在することが確認可能である(b)。

ており，その血管描出能は通常装置に比し優れていることは明白である。造影検査を繰り返して施行し得た症例における微小血管の再現性も良好で，血管新生療法前後における新生血管の評価に関しても，本装置を用いることにより，既存の装置では得られない微小血管レベルでの評価が可能と思われる。

おわりに

病院設置型微小血管造影装置を用いることにより50μm前後の微小血管が観察可能であり，その安全性や再現性についても臨床上問題はなかった。末梢動脈閉塞症に対する血管新生療法により，微小側副血管がどのように発達促進するのか，その解明には今後の症例の積み重ねが必要である。

●文　献

1) Mori H, Hyodo K, Tobita K, et al : Visualization of penetrating transmural arteries *in situ* by monochromatic synchrotron radiation. Circulation 89 : 863-871, 1994
2) Takeshita S, Isshiki T, Mori H, et al : Use of synchrotron radiation microangiography to assess development of small collateral arteries in a rat model of hindlimb ischemia. Circulation 95 : 805-808, 1997
3) Takeshita S, Isshiki T, Ochiai M, et al : Endothelium-dependent relaxation of collateral microvessels

after intramuscular gene transfer of vascular endothelial growth factor in a rat model of hindlimb ischemia. Circulation 98 : 1261-1263, 1998

4) Tateishi-Yuyama E, Matsubara H, Murohara T, et al, Terapeutic Angiogenesis using Cell Transplantation (TACT) Study Investigators : Therapeutic angiogenesis for patients with limb ischemia by autologous transplantation of bone-marrow cells ; a pilot study and a randomised controlled trial. Lancet 360 : 427-435, 2002

5) Tanioka K : A highly sensitive camera tube using avalanche multiplication in an amorphous selenium photoconductive target. Proc SPIE Int Soc Opt Eng 1656 : 1-12, 1992

6) Kubota M, Kato T, Suzuki S, et al : Ultrahigh-sensitivity new super HARP camera. IEEE Trans Broadcasting 42 : 251-258, 1996

7) Umetani K, Ueki H, Takeda T, et al : High-spatial-resolution and real-time medical imaging using a high-sensitivity HARPICON camera. J Synchrotron Radiat 5 : 1130-1132, 1998

8) Tanioka K, et al : Ultra-high-sensitivity New Super-HARP Pickup Tube. IEEE Workshop on CCD and Advanced Image Sensors, 2001

Am J Physiol Heart Circ Physiol 288: H1444–H1450, 2005.
First published November 11, 2004; doi:10.1152/ajpheart.00266.2004.

Adrenomedullin enhances therapeutic potency of bone marrow transplantation for myocardial infarction in rats

Takafumi Fujii,[1] Noritoshi Nagaya,[2,3] Takashi Iwase,[2] Shinsuke Murakami,[2] Yoshinori Miyahara,[1] Kazuhiro Nishigami,[3] Hatsue Ishibashi-Ueda,[5] Mikiyasu Shirai,[1] Takefumi Itoh,[2] Kozo Ishino,[6] Shunji Sano,[6] Kenji Kangawa,[4] and Hidezo Mori[1]

Departments of [1]Cardiac Physiology, [2]Regenerative Medicine and Tissue Engineering, [3]Internal Medicine, [4]Biochemistry, and [5]Pathology, National Cardiovascular Center, Osaka; and [6]Department of Cardiovascular Surgery, Okayama University Medical School, Okayama, Japan

Submitted 18 March 2004; accepted in final form 19 October 2004

Fujii, Takafumi, Noritoshi Nagaya, Takashi Iwase, Shinsuke Murakami, Yoshinori Miyahara, Kazuhiro Nishigami, Hatsue Ishibashi-Ueda, Mikiyasu Shirai, Takefumi Itoh, Kozo Ishino, Shunji Sano, Kenji Kangawa, and Hidezo Mori. Adrenomedullin enhances therapeutic potency of bone marrow transplantation for myocardial infarction in rats. *Am J Physiol Heart Circ Physiol* 288: H1444–H1450, 2005. First published November 11, 2004; doi: 10.1152/ajpheart.00266.2004.—Adrenomedullin (AM), a potent vasodilator, induces angiogenesis and inhibits cell apoptosis through the phosphatidylinositol 3-kinase/Akt pathway. Transplantation of bone marrow-derived mononuclear cells (MNC) induces angiogenesis. We investigated whether infusion of AM enhances the therapeutic potency of MNC transplantation in a rat model of myocardial infarction. Immediately after coronary ligation, bone marrow-derived MNC (5×10^6 cells) were injected into the ischemic myocardium, followed by subcutaneous administration of 0.05 $\mu g \cdot kg^{-1} \cdot min^{-1}$ AM (AM-MNC group) or saline (MNC group) for 3 days. Another two groups of rats received subcutaneous administration of AM alone (AM group) or saline (control group). Hemodynamic and histological analyses were performed 4 wk after treatment. Cardiac infarct size was significantly smaller in the MNC and AM groups than in the control group. A combination of AM infusion and MNC transplantation demonstrated a further decrease in infarct size. Left ventricular (LV) maximum change in pressure over time and LV fractional shortening were significantly improved only in the AM-MNC group. AM significantly increased capillary density in ischemic myocardium, suggesting the angiogenic potency of AM. AM infusion plus MNC transplantation demonstrated a further increase in capillary density compared with AM or MNC alone. Although MNC apoptosis was frequently observed 72 h after transplantation, AM markedly decreased the number of terminal deoxynucleotidyl transferase-mediated dUTP nick-end labeling-positive cells among the transplanted MNC. In conclusion, AM enhanced the angiogenic potency of MNC transplantation and improved cardiac function in rats with myocardial infarction. This beneficial effect may be mediated partly by the angiogenic property of AM itself and by its antiapoptotic effect on MNC.

angiogenesis; apoptosis; mononuclear cell

DESPITE THE RECENT REMARKABLE progress in medical and surgical treatment for ischemic heart disease, this disease remains a major cause of death worldwide (5). Bone marrow-derived mononuclear cells (MNC) contain various kinds of cell lineages and numerous cytokines that contribute to neovascularization (1, 15). In fact, autologous transplantation of bone marrow cells has been shown to enhance angiogenesis and improve cardiac function in an animal model of cardiac ischemia (6, 9, 10). Recent human studies have demonstrated beneficial effects of transplanted MNC in patients with ischemic heart disease (23, 25). However, some patients fail to respond to this cell therapy. Thus a novel therapeutic strategy to enhance the angiogenic property of MNC is desirable.

Adrenomedullin (AM) is a potent vasodilator peptide that was originally isolated from human pheochromocytoma (8). We have shown that infusion of AM has beneficial hemodynamic and renal effects in patients with heart failure (17). On the other hand, AM has been shown to activate the phosphatidylinositol 3-kinase (PI3-kinase)/Akt-dependent pathway in vascular endothelial cells, which is considered to regulate multiple critical steps in angiogenesis including endothelial cell proliferation, migration, and capillary-like formation (14, 22). In fact, we have shown that AM gene transfer induces therapeutic angiogenesis in a rabbit model of hindlimb ischemia via activation of Akt (24). These findings suggest that AM may play an important role in the regulation of vascular regeneration. In addition, AM has been shown to exert an antiapoptotic effect on a variety of cells including vascular endothelial cells (7, 20). Taking these findings together, combination therapy with MNC transplantation and AM infusion may have additional or synergetic effects on therapeutic angiogenesis for the treatment of ischemic heart disease.

Thus the purposes of this study were *1*) to investigate whether infusion of AM enhances the angiogenic potency of MNC transplantation in a rat model of myocardial infarction, and *2*) to investigate the effects of AM on survival and differentiation of the transplanted MNC to examine the underlying mechanisms of the effects induced by AM.

MATERIALS AND METHODS

Animal model. Myocardial infarction was produced in male Lewis rats weighing 200–220 g by left coronary ligation. In brief, after rats were anesthetized by intraperitoneal injection of pentobarbital sodium (30 mg/kg body wt), they were ventilated artificially. The heart was exposed via left thoracotomy, and the left coronary artery was ligated 2–3 mm from its origin between the pulmonary artery conus and the left atrium using a 6-0 proline suture. Finally, the heart was restored to its normal position, and the chest was closed. The Animal Care Committee of the National Cardiovascular Center approved this experimental protocol.

Address for reprint requests and other correspondence: N. Nagaya, Dept. of Regenerative Medicine and Tissue Engineering, National Cardiovascular Center Research Institute, 5-7-1 Fujishirodai, Suita, Osaka 565-8565, Japan (E-mail: nnagaya@ri.ncvc.go.jp).

The costs of publication of this article were defrayed in part by the payment of page charges. The article must therefore be hereby marked "*advertisement*" in accordance with 18 U.S.C. Section 1734 solely to indicate this fact.

Preparation of MNC. After Lewis rats were killed, bone marrow from the femur and tibia was collected and put in PBS. Marrow cells were loaded on a 1.077 gradient of Ficoll (Lymphoprep; Nycomed Pharma, Oslo, Norway) and centrifuged at 1,500 rpm for 20 min. The cells were then washed with 10 ml PBS to remove the Ficoll and centrifuged at 2,000 rpm for 10 min. The cells were finally suspended in PBS at a concentration of 5×10^6 cells in 50 μl PBS for transplantation. Fluorescence-activated cell sorting analysis demonstrated that 22 ± 1% of MNC were positive for lectin from ulex europaeus (UEA)-1 lectin (Sigma, St. Louis, MO).

MNC transplantation and AM infusion. Transplantation of bone marrow-derived MNC and/or 3-day infusion of AM was performed immediately after coronary ligation. MNC (5×10^6 cells in 50 μl PBS) were injected into the myocardium at five points in the border zone surrounding the infarct by using a 27-gauge needle. Recombinant human AM (0.05 $\mu g \cdot kg^{-1} \cdot min^{-1}$) was subcutaneously administered by using an osmotic minipump (model 2004; Alza, Palo Alto, CA) for 3 days. The pump was positioned in a pocket constructed in the subcutaneous tissue just below the subscapular region. For control, 5% glucose was infused in a similar manner in the rats receiving coronary ligation. This protocol resulted in the creation of four groups: *1*) AM infusion plus MNC transplantation (AM-MNC group, $n = 15$), *2*) vehicle infusion plus MNC transplantation (MNC group, $n = 14$), *3*) AM infusion plus PBS injection (AM group, $n = 14$), and *4*) vehicle infusion plus PBS injection (control group, $n = 13$).

Echocardiographic studies. Echocardiographic studies were performed 4 wk after surgery using a 7.5-MHz phased-array transducer (model HP SONOS 5500; Hewlett-Packard, Andover, MA). Rats were anesthetized by intraperitoneal injection of pentobarbital sodium (30 mg/kg body wt) as a supplement to maintain mild anesthesia. M-mode tracings were obtained at the level of the papillary muscles. Anterior and posterior end-diastolic wall thickness, left ventricular (LV) end-diastolic and end-systolic dimension, and LV fractional shortening were measured from three consecutive cardiac cycles by the American Society for Echocardiology leading-edge method (21).

Cardiac catheterization. Cardiac catheterization was performed 4 wk after surgery. Rats were anesthetized with intraperitoneal pentobarbital and placed on a heating pad to maintain body temperature at 37–38°C throughout the study. A 1.5 Fr micronanometer-tipped catheter was inserted in the right carotid artery for measurement of heart rate and mean arterial pressure. The catheter was then advanced into the LV for measurement of LV end-diastolic pressure and then replaced with a thermomicroprobe for measurements of cardiac output. These hemodynamic variables were measured with a pressure transducer (UFI, Morro Bay, CA) connected to a polygraph and recorded with a thermal recorder (model 7758 B system; Hewlett-Packard).

Infarct size measurement. After completion of hemodynamic measurements, the heart was arrested by an injection of 2 mmol KCl through the carotid artery, and the cardiac ventricles were excised. The size of myocardial infarction was determined by a previously described method (2). In brief, incisions were made in the LV so that the tissue could be pressed flat. The circumference of the entire flat LV and the visualized infarcted area, as judged from both the epicardial and endocardial sides, was outlined on a clear plastic sheet. The difference in weight between the two marked areas on the sheet was used to determine infarction size and was expressed as a percentage of LV surface area.

Histological analysis of microvessel density. LV myocardium was fixed in 10% formalin. Three cross sections of the LV, cut from apex to base, were obtained from individual rats for comparison among four groups ($n = 5$ each). They were embedded in paraffin and stained with Masson's trichrome for measurement of interstitial fibrosis. In other rats ($n = 5$ each), LV myocardium was embedded in optimum cutting temperature (OCT) compound (Sakura Finetechnical, Tokyo, Japan), snap frozen in liquid nitrogen, and cut into 5-μm-thick sections. Tissue sections were stained for alkaline phosphatase with an indoxyltetrazolium method to detect capillary endothelial cells ($n = 5$ in each group). The number of capillary vessels was counted in the peri-infarct area (a 1.0-mm band next to the scar) excluding scar region using a light microscope at a magnification of ×200. The numbers in five high-power fields in each rat were averaged and expressed as the number of capillary vessels. These morphometric studies were performed by two examiners who were blinded to treatment.

Detection of MNC apoptosis. To examine the antiapoptotic effect of AM on transplanted MNC, red fluorescence-labeled MNC were transplanted into ischemic myocardium in rats with ($n = 5$) and without ($n = 5$) AM infusion. Before implantation into the ischemic heart, suspended MNC were labeled with fluorescent dyes with a PKH26 (Red Fluorescent Cell Linker Kit; Sigma), as reported previously (13). AM was subcutaneously administered by using a minipump for 3 days. Rats were killed 72 h after MNC transplantation. The LV was enucleated, and muscle samples were embedded in OCT compound and snap frozen in liquid nitrogen for the detection of apoptosis. Serial sections of the heart were stained by terminal deoxynucleotidyl transferase-mediated dUTP nick-end labeling (TUNEL) for apoptosis using an in situ apoptosis detection kit (model S7111 Apoptag Fluorescein Kit; Intergen). Apoptosis of transplanted MNC was also evaluated by the detection of cleaved caspase-3-positive cells. In brief, the frozen tissue sections were incubated with anticleaved caspase-3 antibody (Cell Signaling), followed by incubation with FITC-conjugated IgG antibody (BD Pharmingen, San Diego, CA). The number of TUNEL/PKH26 double-positive cells and caspase-3/PKH26 double-positive cells was counted in 10 fields of each rat using a confocal microscopy (Fluoview model 500; Olympus, Tokyo, Japan).

The antiapoptotic effect of AM on MNC was also evaluated by in vitro TUNEL assay. MNC were plated on 12-well plates (1×10^6 cells per well) and cultured in serum-free medium for 24 h with control buffer, AM (1×10^{-7} M), or AM plus wortmannin, a PI3-kinase inhibitor (50 nM). Randomly selected microscopic fields ($n = 10$) were evaluated for calculating the ratio of TUNEL-positive cells to total cells.

Monitoring of implanted MNC in ischemic heart. Additional rats were used to examine whether transplanted MNC differentiate into endothelial cells, cardiomyocytes, vascular smooth muscle cells, or macrophages in the ischemic heart. PKH26 (red fluorescence)-labeled MNC were injected into the ischemic heart in rats with ($n = 8$) and without ($n = 8$) AM infusion. These subgroups of rats were killed 4 wk after coronary ligation. To identify vascular endothelial cells in vivo, FITC-labeled UEA-1 lectin was intravenously administered 30 min before the rats were killed ($n = 5$ in each group). The LV was enucleated, and muscle samples were then embedded in OCT compound, snap frozen in liquid nitrogen, and cut into sections. Sections were counterstained with 4′,6′-diamidino-2-phenylindole (DAPI) to detect nuclei. The number of DAPI/PKH26 double-positive cells and lectin-positive cells in the peri-infarct area was counted in 10 fields of each rat using a confocal microscopy. Frozen sections from other rats ($n = 3$ in each group) were incubated with mouse anticardiac troponin T (Novocastra, Newcastle, UK), anti-α-smooth muscle actin antibody (Dako, Copenhagen, Denmark), and anti-ED1 antibody (Serotec, Oxford, UK), followed by incubation with FITC-conjugated IgG antibody. In other rats (MNC group, $n = 5$; AM-MNC group, $n = 5$), the cardiac muscle from base to apex was transversely cut into 6-μm slices to calculate the number of transplanted MNC present within the heart 4 wk after transplantation. These morphometric studies were performed by two examiners who were blinded to treatment.

Statistical analysis. Numerical values were expressed as means ± SE. Comparisons of parameters among the four groups were performed by one-way ANOVA, followed by Newman-Keuls test for unpaired data. Comparisons of parameters between two groups were made by unpaired Student's *t*-test. A value of $P < 0.05$ was considered significant.